A monolithic compliant microgripper for UW RoboFly

Suvesha Chandrasekaran

A thesis
submitted in partial fulfillment of the
requirements for the degree of

Master of Science in Mechanical Engineering

University of Washington

2022

Committee:

Jeffrey Ian Lipton, Chair

Sawyer B Fuller

Lucas Meza

Program Authorized to Offer Degree:
Mechanical Engineering

University of Washington

Abstract

A monolithic compliant microgripper for UW RoboFly

Suvesha Chandrasekaran

Chair of the Supervisory Committee:
Professor Jeffrey Ian Lipton
Mechanical Engineering

Compliant structures reduce part counts and are easier to assemble at micro and meso- scales as compared to their rigid counterparts. In this work, we design and prototype in-plane bendable flexures to build a compliant microgripper. We use pop-up lamination hinges made from nitinol and laminated with FR-4 sandwiches, to induce directional stiffness in the flexures. This enables the flexures to predominantly bend in-plane. These compliant composite flexures are capable of taking 10 times their weight and are laser micro-machined using a nano-laser with short pulse width. Ultimately we build a miniature straight line mechanism such as the lagged lambda to demonstrate the working and the capability of these flexures. One application shown in this work is a compliant monolithic microgripper that is light enough to be mounted on the UW RoboFly for purposes such as sensor dropping from the flapping wing robot[1] or to pre-emptively charge aerial vehicles through a wire from the gripper.

TABLE OF CONTENTS

LIST OF FIGURES

GLOSSARY

FLEXURE JOINTS: These joints connect two rigid links with an elastic member.

FAILURE ANGLE: Angular deflection of the blade flexure at which the beam break, de-laminates or shows plastic deformation

LOADING CYCLE: Each loading cycle applies a concentrated point load at one end of the beam using a pair of tweezers to deflect the beam up to a fixed angle that is below its failure angle. The cycle is run maximum of 50 times per flexures

ACKNOWLEDGMENTS

I would like to thank my advisors Dr. Jeffrey Ian Lipton and Dr. Sawyer Fuller, for their continued support, patience and invaluable advice. I would also like to thank my colleague and friend Ian Good for his keen insights and Dr. Vikram Iyer & Dr. Lucas Meza for their valuable suggestions that shaped my thesis.

DEDICATION

This thesis is dedicated to my sister Pravesha. Thanks for all the cheer and support.

Chapter 1

INTRODUCTION

1.1 Motivation

The advancement in micro-scale and nano-scale science and technology has created a demand for high impact applications in healthcare, manufacturing, sensor networks, etc. Consequently,micro systems have evolved to to be able to access small spaces within human body with precision and dexterity [2] [3]. A major advantage of compliant mechanism is the reduction in part count while building mechanisms. This feature becomes especially useful in micro-robotics considering the size of the robot and the ease of assembly. Not to mention the cost of the robot reduces with reduced part count. Thus, scaling down compliant mechanisms poses a possibility of building insect scale applications with simple designs and easier assembly. With the increase in soft robotic applications in the field of healthcare [4] , this work's original vision was to build a miniature soft robotic endoscopy attachment unlike the guide wire technique used today [5].

Existing technology at macroscopic scale, like a remotely operated vehicle (ROV) cannot be scaled down [6], while guide wires and passive heads have limited (or in some cases) no directional control [7]. Handed Shearing Auxetic (HSA)[8] offer the unique possibility of building flexible structures and the ability to control the steerable head [9].However, we quickly ran into miniaturisation issues when we attempted to downsize a full HSA tube. We thus chose to build individual miniature flexures with high directional deflections, that could be tiled to build a variety of compliant mechanisms at insect scale- opening up a host of insect scale applications not limited to a steerable catheter tip - with this work as the ground for future applications.

1.2 Background

A compliant mechanism is a flexible mechanism that achieves motion by way of elastic deformation. Most moving things in nature are flexible instead of stiff, and the motion comes from bending the flexible parts [10]. Thin, long, monolithic flexures are frequently used to guide motion by using the structure's predictable elasticity [11] [12]. To maximise the in-plane bending to out of plane bending ratio, we employed a lamination technique, thereby inducing directional stiffness [13]. Multi joint pop-up robot like the HAMR-Jr [14] use the relative motion between flexures akin to produce a walking mechanism akin to a roach. Microgrippers have also used similar relative motion between the flexures to grip onto items. Laser cut nickel microgripper were designed to utilize multi-cascades approach to act as microtweezers and were actuated with an electrothermal effect giving a maximum displacement of 30 µm and were 2.8mm long and 1.4mm wide. [] One of the earlier monolithic flexure based microgripper was cut from a single piece of spring steel or aluminium using Electron Discharge machining (EDM) and was in the size rage of 200-800 µm [11] A two fingered planar compliant microgripper used revolute or prismatic joints to grip onto items using a linear actuating element as a shape memory spring. [12]

1.3 Main Contribution

. This work focuses on downsizing existing in-plane bendable flexures to build monolithic, complaint micro-scale mechanisms. We designed and prototype the aforementioned flexures and characterised them based on their geometric parameters. Each individual flexure was stacked on top of one another sandwiched between a stiffness increasing material- to build a pop-up laminated structure [13]. This provides directional stiffness and minimize out-of-plane bending. Tilable mechanisms give us an increased density of mechanism, for eg: strandbeest;This is one of the reasons why we prefer to bend inplane as it predominantly tiles laterally and this is helpful at small scale. Over the course of the design process of the flexure, different flexure geometries and widths were compares to finalize a single optimised flexure design. We concur that a blade flexures with a beam width of 100 µ m and a sandwich lamination with FR-4 in between two layers of nitinol

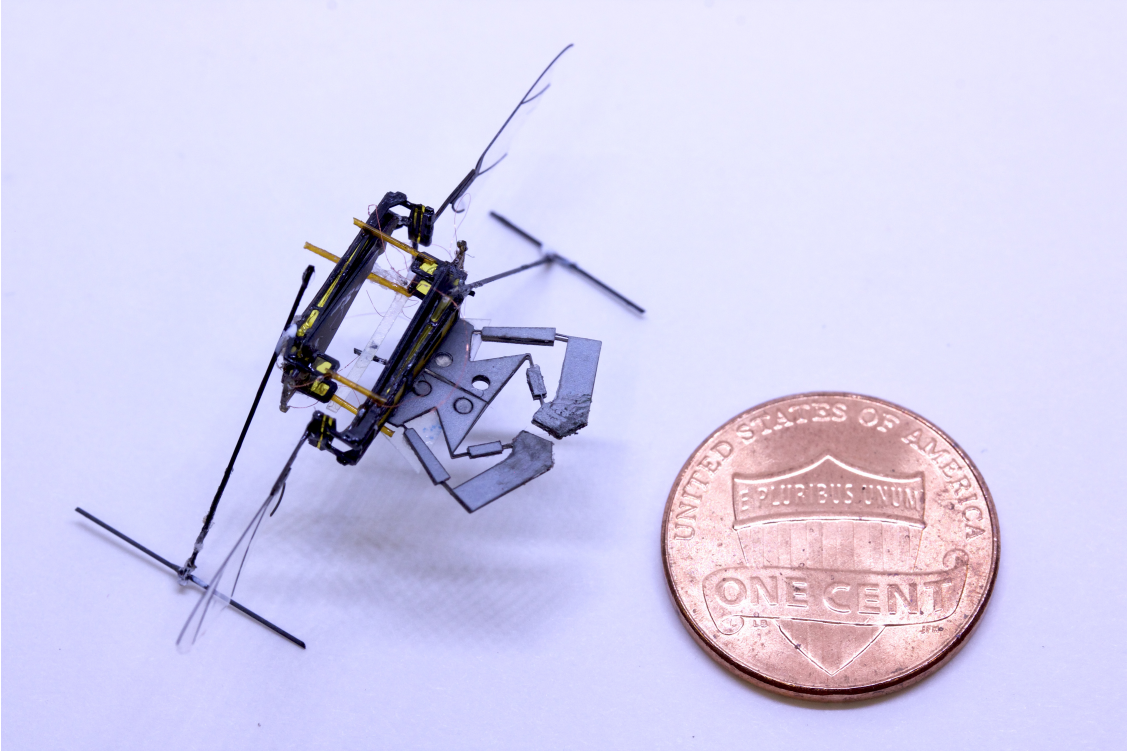

Figure 1.1: A monolithic compliant microgripper on the UW Robofly. The gripper has a payload of 7 gms minimum and can widen up to 2 mm

provide strength in the axial direction while maintaining 45 degrees of in-plane angular elastic deformation. To demonstrate the working of the flexure mechanism, a straight line mechanism called the chebyshev's lagged lambda was used for the compliant monolithic microgripper. Each half of the pincer can hold upto 7 gms weight and the pincer can widen up to 2 mm. The size of the microgripper is 7.24 x 9.7 mm.

Chapter 2

SYSTEM DESIGN

2.1 Overview

We begin by designing individual flexures optimised for in-plane bending, subsequently the out of plane bending is constrained. We employ two major strategies to achieve this end goal. Firstly, we build individual flexures with thin, long cross sectional areas with a thickness:width aspect ratio of 1:1. Each individual layer is then laminated by layering each flexure on top of another to obtain stiffness in the axial direction, thereby increasing the thickness:width ratio to 3:1. The resulting high aspect ratio increases stiffness along the out-of-plane axis, minimizing out-of-plane bending.

This section delves further into the design, fabrication and characterisation of the individual flexures. Like all engineering design processes we begin our system design by identifying the design criteria, zeroing in on the material selection, rapid prototyping with a laser cutter,them move to assembly and lamination. We will then delve into the details of the four bar straight line mechanism that was used to build the microgripper and the microgripper design as a whole.

2.2 Design Criteria

Mathematically, from the Euler-Bernoulli's beam bending equation,

$$\frac{d^2}{dx^2}(EI\,\frac{d^2w}{dx^2}) = q$$

where E is the stiffness

From Euler Bernoulli, we can safely assume that the width and the length of the beam are directly related to the beam deflection. The Smaller the beam width, greater the beam bending. Thus our basic criteria for flexure form is a thin, long beam with low width:length ratio.

To decide the geometry of the flexure we analyze the different methods in which a flexure can

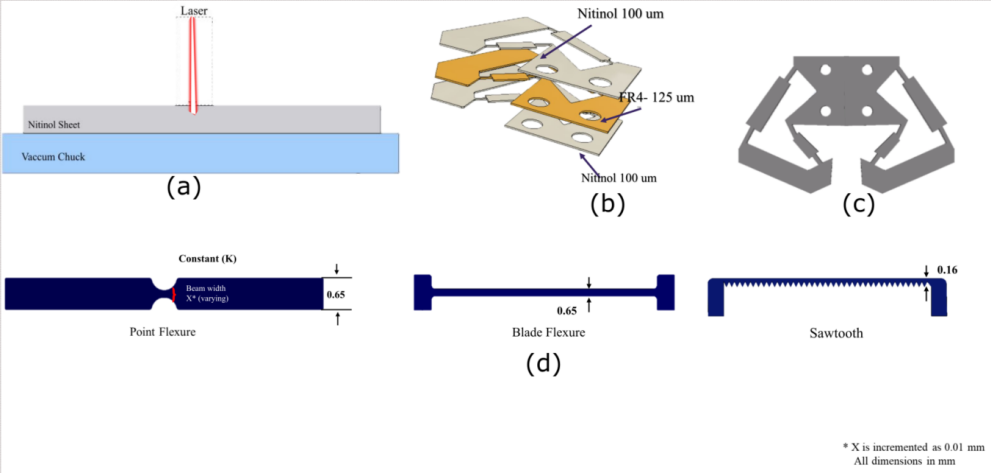

Figure 2.1: Individual flexures are micro machined using a UV laser (a) Individual layers are then laminated by sandwiching one layer of 100 µm thick FR-4 between 2 layers of 100 µm thick nitinol sheets to build directional stability as shown in (b). Inset in (b) shows the side view of the lamination. Individual flexures were tested out for different geometries namely, blade flexure, point flexure and saw-tooth flexure as shown in (c). The fully assembled microgripper is shown in (d)

happen. predominantly there are three types of flexures:

- Pin flexure- a thin bar or cylinder of material, constrains 3 degree of freedom when geometry matches a notch cutout.(See figure 2(d))
- Blade flexure- thin sheet of material, constrains 3 degrees of freedom.(see figure 2(d))
- Notch flexure- thin cutout on both sides of a thick piece of material, constrains 5 degrees of freedom.

For this work, we can eliminated notch flexures since they didn't yield in-plane bending at 100 µ m thickness and width

Since there are two variables to the beam design (length, width of cross-section). We begin by constraining the effect of beam length to understand the role and range of motion obtained by modifying the beam width. This is done by build pin flexures and characterising them. Once the

beam widths give a range of in-plane bending for each cross sectional width, we go ahead and build line flexures for aforementioned widths.

2.2.1 Pin Flexure

We employ a dog-bone inspired structure with a reduced cross section in the center as shown in figure 2.1 (c) to focus all the bending moment at a single point. We chose to empirically find the thickness of cross-section of the flexure to fix the upper and lower limits of the cross section, that enables in-plane bending. We added fillets of radius of 0.23 mm to each sharp corner to reduce stress concentrations. The baton cross-section varied from a lower limit of 60 µm to an upper limit of 200 µm. It is to be noted that the 60 µm cross-section shows the maximum in-plane deflection while the 200 µm shows no in plane deflection. The in-plane deflection stops at about 160 µm

2.2.2 Blade Flexure

For large scale beam deflection problems, the moment of inertia (I) is inversely proportional to the beam deflection. MI depends on the beam width and even more importantly, on the beam geometry. The further the mass is concentrated from the neutral axis, greater is the moment of inertia by definition of moment of Inertia. A saw-tooth flexure shows greater pliability than a pure flexure owing to the geometry of the former. This was also taken into consideration while building the blade flexure. First, a simple long flexure with support structures at the end, as shown in figure 2.1 (d) was designed and machined. The deflection of a simple blade flexure was compared against that of the saw-tooth on parameters such as maximum deflection, and the deflection cycle withstood by both the geometries. On further investigation, we quickly realised that while incorporating the saw tooth in the flexure gave significantly high bending angles for individual layers, the stress concentration at the saw tooth broke the beam easily. It was also noticed in the subsequent lamination that it was difficult to align the teeth of the saw tooth geometry to build the laminate, since the feature size of the saw tooth was about 20 µm in length and width. We discarded the idea of incorporating saw tooth into the flexures owing to the aforementioned reasons. Instead we selected a simple

long flexure as shown in figure 2.1(d), with a thickness of 100 μM and flexure width and length as 0.1 mm and 7 mm respectively.

2.3 Material selection

To obtain proof of concept to validate our in-plane bending hypothesis we chose to run the preliminary test on the economical, easily available copper clad FR-4.The FR-4's sufficient deflection and our rapid iterations on it, built the ground work for actual flexure micro-machining. A basic look at available material categories can summarise the following for us:
1. Metals, exhibit high elastic modulus but are not suitable for large scale beam deflection.
2. Rubbers and plastic are easily deformable but quickly lose the ability to return to their original shape on removal of the deforming load. Now, super alloys deform elastically up to 10% strain, and can withstand significant directional loads depending on composite layup and base material.
One such super elastic material is Nitinol. It can deform 10-30 times more than its metallic counterparts. with the goal to exploit this property we chose commercially available super elastic Nitinol sheet with a thickness of 100 μM. It is to be noted that the thickness of FR4 used in our preliminary tests was also 100 μ.

2.4 Four-bar mechanisms

Once we built individual flexures and validated their properties as stated in section IV of this paper, we employed the in plane bending property of the aforementioned flexures to build a compliant straight line mechanism called the Chebyshev lambda mechanism.The lambda mechanism is a simple four bar linkage that converts rotational motion to approximate straight line motion.

2.5 Microgripper

2.5.1 microgripper

We demonstrate an application of this lambda mechanism by using it to design a microgripper. To build the microgripper, we aligned two lambda mechanisms, such that they mirror each other,

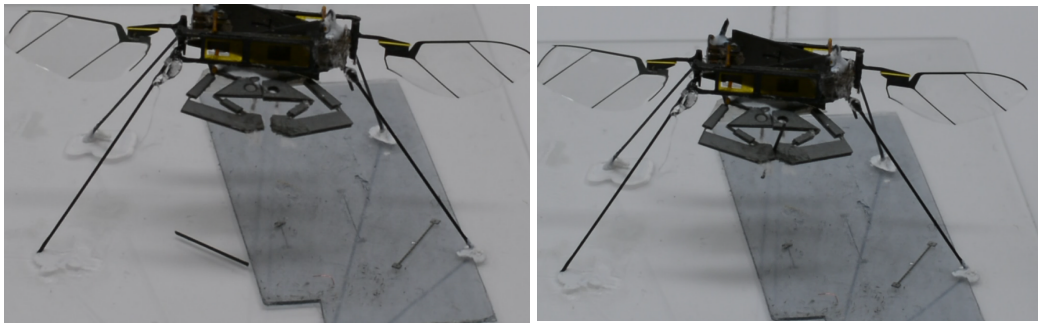

Figure 2.2: (a) shows the compliant microgripper mounted onto the robofly in its open state. (b) On applying pull forces to the gripping arms, the ends of the microgripper close to grip onto an object

as shown in figure 2.1(c). Each lambda mechanism formed one half of the micro gripper. The lower limbs of the micro gripper were fitted with tiny carbon fiber sheets with a slit to secure the sheet to the gripper. The Carbon fiber sheets acted as grasping pads on the microgripper. While there are different ways to actuate this mechanism, we chose a simple solenoid based actuation to demonstrate the functionality of the microgripper. Using Micron-Wing's solenoid based hinge actuator, we attached a taut thread to the two ends of the micro gripper and secured the other end on the solenoid actuator using Cyanoacrylate. On energising the solenoid, the threads gets pulled by the hinges. Since the other end is rigidly secured to the tips of the microgripper, the ensuing motion pulls the microgripper to give us a pincer like movement. In the absence of the pull force the gripper stays in open state. Figure 2.2(a) and 3(b) show the open an closed state of the microgripper.

Chapter 3

METHODS

3.1 Nitinol- material characteristics

Nitinol is a super alloy of nickel and titanium with near equiatomic composition.The alloy exhibits high flexibility owing to its wide recoverable strain range of up to 10 %, in which the stress is kept low [15]. We exploit this high elasticity of nitinol to build thin, long flexures by maximizing it's deflection in-plane

3.2 Pin Alignment

We laser micromachine the flexures using a 2 W UV diode pumped solid state (DPSS) laser (Photomachining, Inc., Pelham, MA). It is a nano laser which is of cutting all of the required materials and allows for rapid prototyping and iteration. Laser produces a heat affected zone which can damage the thin flexures. To minimize this effect we vary the laser power and cutting speed. Cutting at the laser's resonant frequency which gives maximum power output guaranteed a quick, clean cut for the 100 µm thick sheets. One cycle of 50 passes with a laser output power of 0.85 - 1.5 W was the recipe we used to cut individual hinges that are 100 µthick. It is important to note that, for the sheets with the same thickness as mentioned above, as the flexure width reduces below 100 µm, it is imperative to cut at lower power to avoid burrs and to reduce residual thermal stresses on the beam flexure.

To facilitate precise alignment of the individual lamina we employ a technique called pin alignment. We cut coupons of individual flexure with scaffolding to hold the coupons to their base material between two precisely aligned horizontal holes. These holes are positioned to align with a stainless steel plate to create a layup. The top and bottom layers of the layup are cut using Nitinol

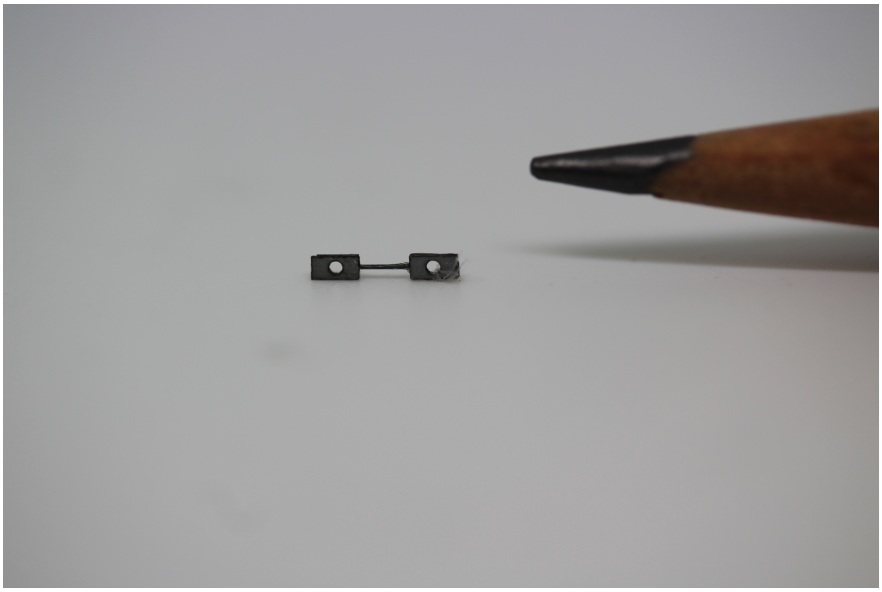

Figure 3.1: Laminated flexures near a pencil tip for scale

and the middle layup is cut on an FR-4 sheet. The layers are then stacked on the steel plate using two pins on either holes to hold the layers.A thin layer of cyanoacrylate is applied to bond the layers to together. A small piece of gel pack is used in between the steel plate and the layup to prevent them from sticking to the plate. The setup is finished by mounting another steel plate at the top to to apply pressure to the coupons.

Once the individual layers are bonded, we slowly remove the layup from the steel plate and perform a release cut on them using the DPSS laser cutter. With the help of pre-positioned coordinates and markers on the top layer, we preserve the integrity of the release cut such that laminated flexures are separated from the scaffolding.

3.3 Heat Affected Zone

Heat Affected zone (referred as HAZ henceforth) is defined as the non-melted area around the metal tat has been exposed to high temperature resulting in changes in it's material properties.

[16] Typically, to cut through thick sheets of material, the laser is run in multiple cycles over the same area as this increases the intensity of the laser at a a given region, enabling the laser to cut through the material.This however damages flexures owing to the Heat affected Zone. In case of the flexures, it is difficult to calculate the heat affected zone in the flexure owing to the transient nature of the process as also due to the kerf thickness of the flexures. Hence we chose to analytically model the composite beam and compare deflection values with the empirical beam deflection values. The difference is beam deflection value is attributed to the degeneration of the flexure owing to the Heat Affected zone.

3.4 Experimental setup

The size of our flexures limit the usage of traditional methods employed to obtain flexure characteristics. The setup is thus customized to the size and requirement of these flexures. There are two major characteristics measures in the flexures- angular deformation and stiffness.
Angular deformation can be easily measure in plane by mounting a printable protractor underneath a glass slide. and cantilevering the flexure to the center of the protractor on top of the glass slide. Manual movement of the free end enables one to determine the limit up to which a given flexure of defined beam width is elastic- i.e. shows no sign of deformation.

To calculate experimental stiffness of the flexures, we measured the beam deflection using a laser distance sensor (Keyence IA series) and hung a mass we measured the weight of to within 1 mg using a precision scale (Mettler-Toledo) in a cantilevered arrangement. We plot the predicted and experimental values of the stiffness to understand the stiffness characteristics of the laminates.

3.5 Data Analysis and analytical calculations

From Euler-Bernoulli, we understand that maximum beam deflection for a cantilevered beam is given by:

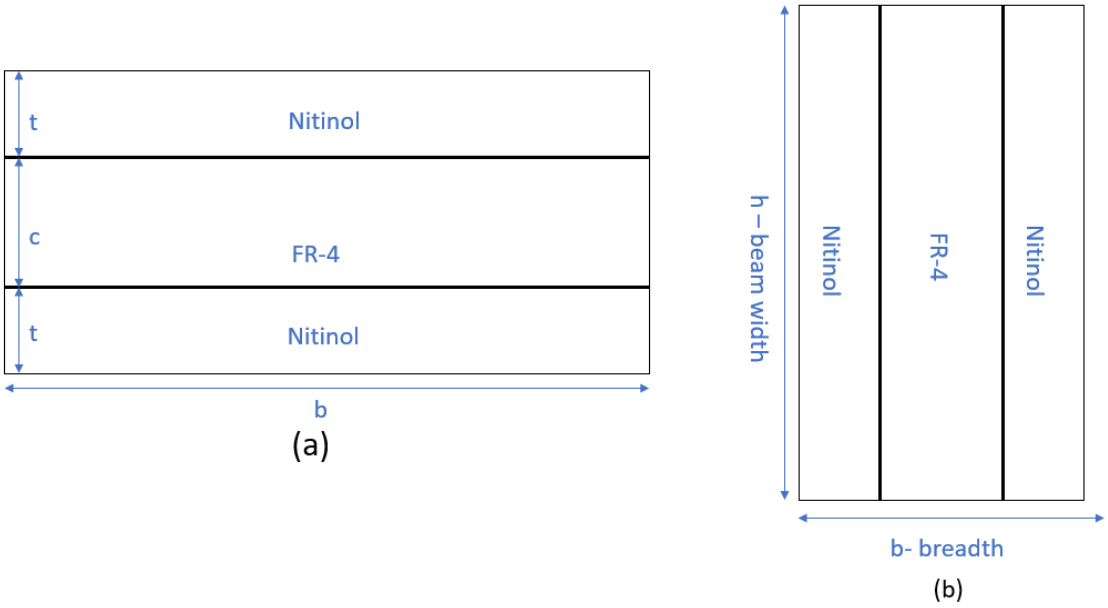

Figure 3.2: Diagrammatic representation of the cross-section of out of plane sandwich panel(a) and in-plane (b). The terms represented in the diagram are enumerated in equations 3.2 and 3.3

$$\delta_{max} = \frac{Pl^3}{3EI} \tag{3.1}$$

where:

P = applied point load at the tip of the free end (in N)

L = length of the beam (in m)

E = Young's Modulus of Elasticity (in Pa)

I = moment of inertia (in m^4)

EI is called the flexural rigidity and it is an indicator of beam stiffness. To compare the stiffnesses of the beams we calculate EI for varying beam widths using (3.1)

The empirical values of beam stiffness are compared with the predicted values of beam stiffness. In the analytical method, we disregard the effect of shear and adhesive forces to simplify the analytical calculation.

A sandwich beam composite has it's out of plane stiffness measured by:

$$EI = \frac{E_{niti} b t^3}{6} + \frac{E_{fr4} b c^3}{12} + \frac{E_{niti} b t}{2}(c+t)^2 \tag{3.2}$$

Parallel axis theorem modification for sandwich panels

where:

EI = equivalent flexural rigidity / stiffness

E_{niti} = young's modulus of nitinol

E_{fr4} = Young's modulus of FR-4

t = thickness of the nitinol lamina

c = thickness of the Fr-4 lamina

b = beam width

For in plane bending, we neglect the effect of shear and calculate EI individually for each layer and consider the lamina to be in parallel to each other. Thus the individual layer stiffnesses are added to obtain total stiffness akin to three springs connected in parallel

We can calculate I for a rectangular cross section as:

$$I = \frac{b h^3}{12} \tag{3.3}$$

where:

b = beam width

h = height of the cross-section

The net stiffness for in-plane beam bending is calculated by:

$$EI = E_1 I_1 + E_2 I_2 + E_1 I_1 \tag{3.4}$$

where:

E_1 = Young's modulus of nitinol

E_2 = Young's modulus of FR-4

I_1 = moment of inertia of top and bottom layer (nitinol)

I_2 = moment of inertia of middle layer (FR-4)

Since FR-4 is an orthotropic material, we consider it's young's modulus perpendicular to the direction of the force applied and neglect to consider the modulus in direction along the force.

Chapter 4

RESULTS

4.1 Experimental Evidence

The goal of the flexure design is to build thin and long flexure that show significant in-plane bending. In our initial experiments we found that the in-plane bending dominant in the region with beam width 60 μm - 200 μm. The UV laser cutter used to micromachine the aforementioned flexures, can cut features as small as 50 μm. We chose 60 μm as the lower limit of the flexure width and increase the width up to 200 μm. We had shortlisted three major flexure geometry and compared their ability to withstand loading and their maximum angular deflection. From figure 4.1 and 4.2, we see that while incorporating the saw tooth in the flexure gave significantly high bending angles for individual layers, the stress concentration in the saw tooth patter broke the beam easily. We thus selected a simple long flexure as shown in figure 2.1, with a thickness of 100 μM and flexure width of 100 μ.

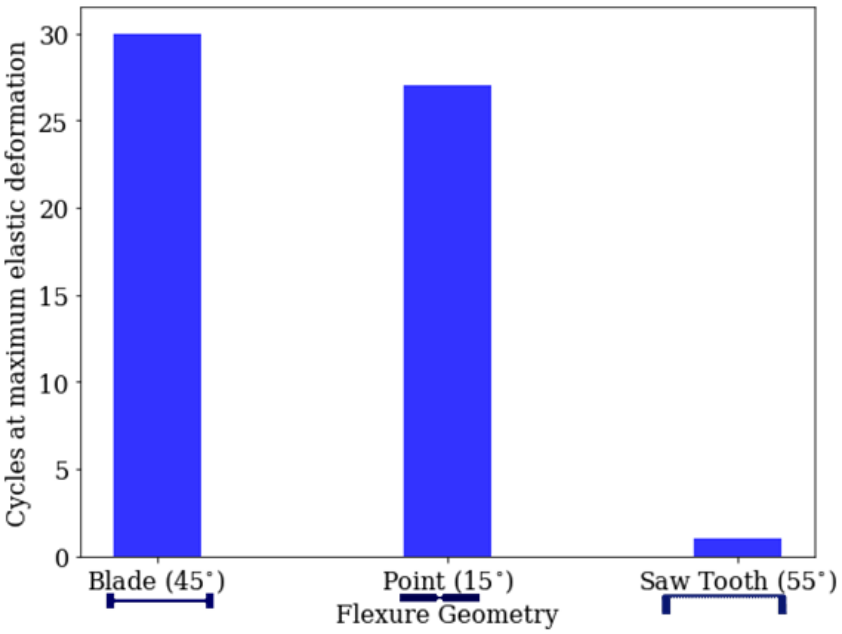

Figure 4.1: Blade flexures withstand the highest amount of fatigue loading when compared to other geometries. Incorporating saw tooth in the blade flexure rapidly brings down the life of the flexure.

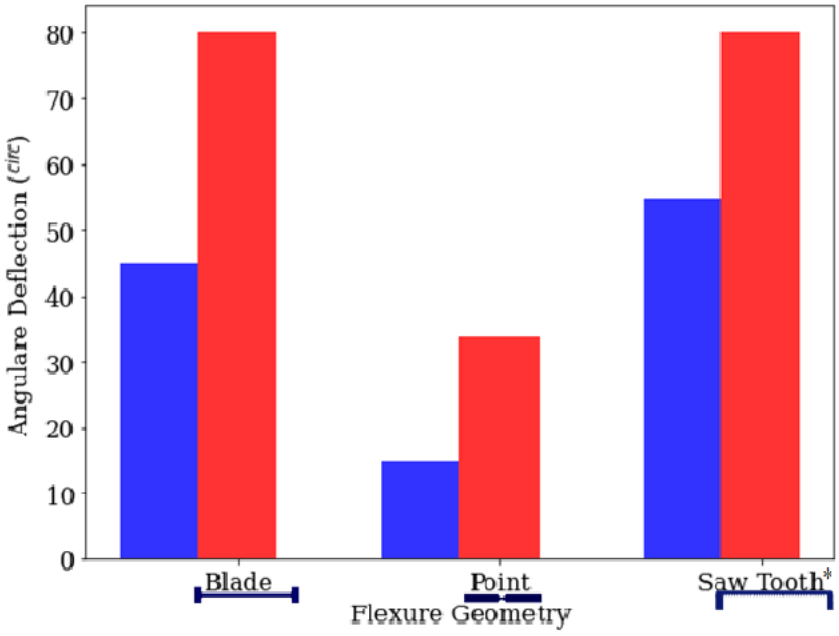

Figure 4.2: The elastic deformation limit and failure angles for different flexure geometries

Laminating the flexures serve two major purposes:

1. They minimize out-of-plane bending of the flexures owing to a high aspect ratio thereby predominantly bending in-plane as shown in figure 6.
2. They vastly increase the ability of the flexures to withstand multiple loading cycles thereby contributing to the life of the flexure as ennumerated in figure 4.3

Since, loading cycles is an indicator of flexure's life, we chose to compare the loading cycles of the flexures before and after lamination Figure 4.2 compares the number of cycles withstood the flexures for a given beamwidth against maximum elastic deflection undergone by the flexure. The laminated flexures withstand higher loading cycles as opposed to their unlaminated counterparts across beamwidths.

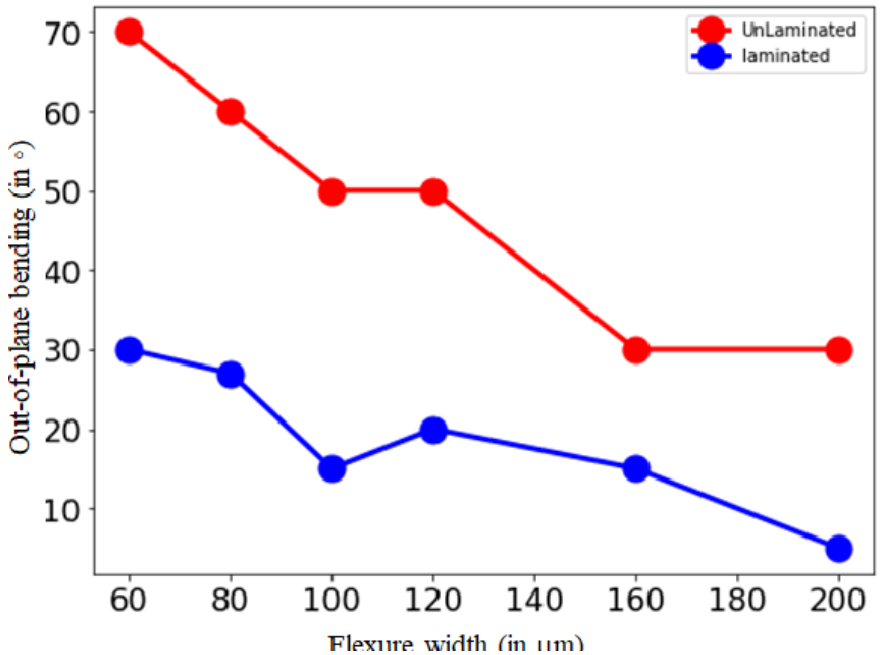

Figure 4.3: Unlaminated flexures have lower stiffness out-of-plane and do not show directional rigidity unlike their laminated counterparts

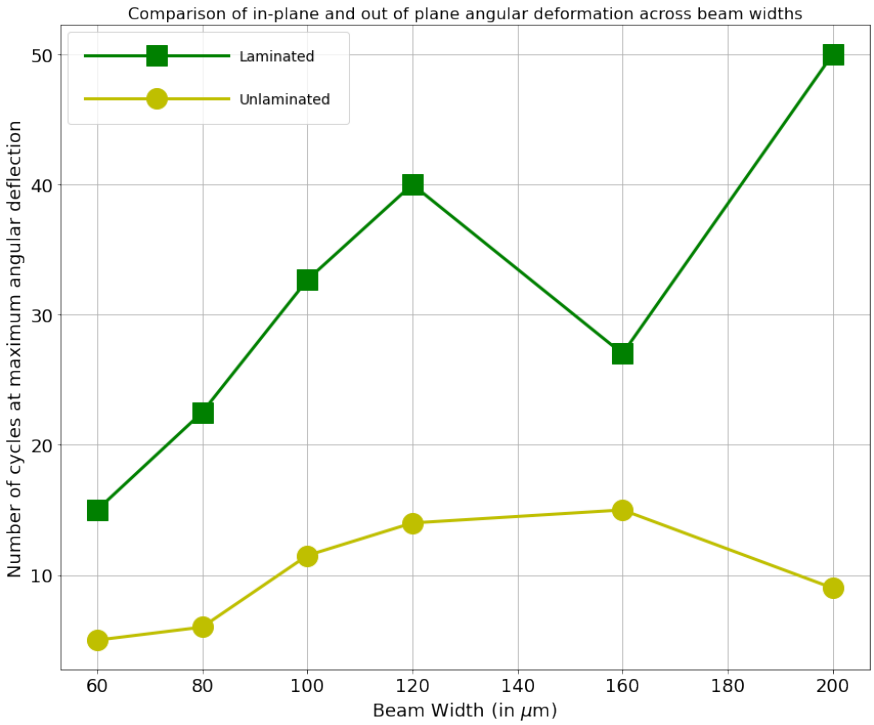

Figure 4.4: Laminated hinges shows higher resilience to fatigue loading as opposed to their non-laminated counterparts. The ability withstand fatigue due to in-plane bending also drastically drops with increasing beam widths in non-laminated hinges unlike laminated ones that remain stable after a certain point.

As per the Euler Bernoulli beam bending, an increase in beamwidth would also contribute to an increase the beam stiffness. A comparison of maximum angular deflection of the beams both, in plane and out of plane across beam widths showed that maximum angular deflection is exhibited just before failing at 100 microns beam width in-plane. The beams also showed relatively lower of out of plane bending amongst other beam widths.Thus we picked the 100 µm M wide flexures, which had reasonable strength while exhibiting up to 45 °of in-plane bending, that was suitable to build our straight line mechanism.

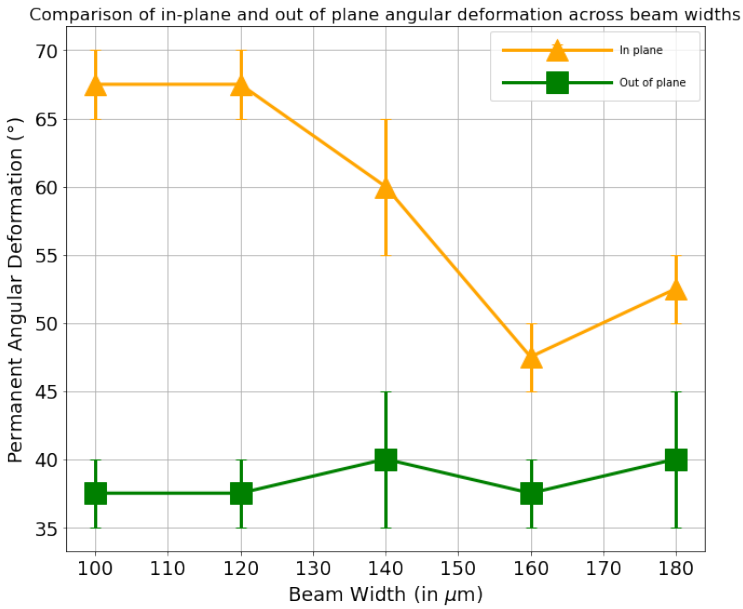

Figure 4.5: The flexure shows maximum angular deformation just before failing at 100 μM indicating high ultimate strength *at near 1:1 aspect ratio*

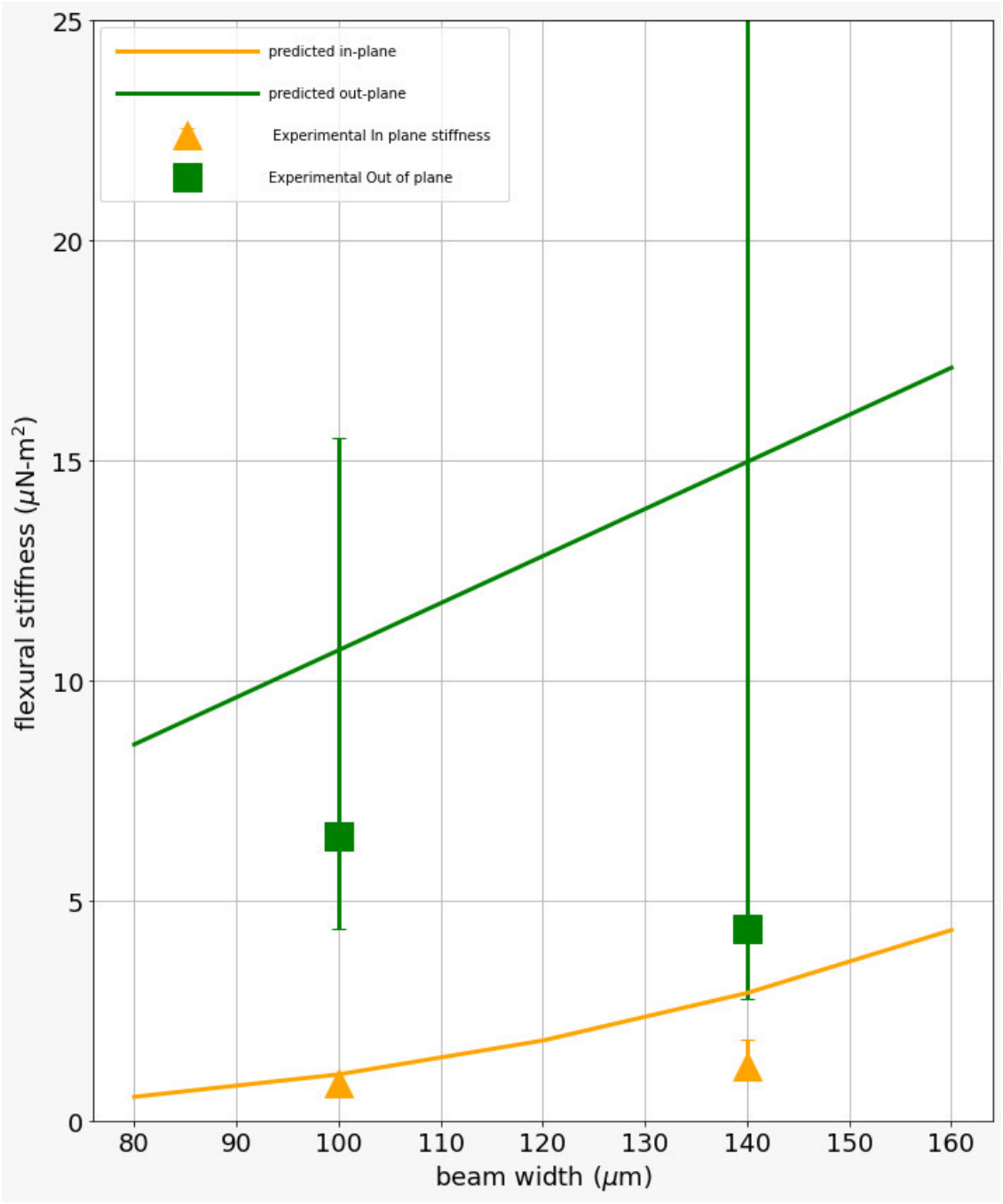

Figure 4.6: The in plane stiffness is much lesser than out of plane stiffness. The predicted values of stiffnesses for both in-plane bending and out of plane bending is higher than the experimental values owing to the shear force between the layers that has been neglected in the calculation of experimental stiffness.

To prove that our flexures are flexible more in plane than out of plane, we calculate the stiffness of the individual coupons by comparing their flexural rigidity - which is a product of their area moment of inertia and young's modulus of elasticity- across varying beam widths. Please note that the actual stiffnesses maybe lower because of the Heat Affected Zone.

4.2 Performance of the micro-gripper

Each half of the micro-gripper are 7 mm x 9 mm in size and they weight 0.04 gms .
When the grippers are fully open the distance between the pincers is 2 mm. Each half of the micro-gripper withstands a minimum payload of 7 gms and withstands 50+ cycles. On the other-hand a non-laminated micro-gripper withstands only 8 cycles.

Chapter 5
CONCLUSION AND FUTURE WORK

This work presents a tilable, laminate Nitinol-Fr4 structure that can be modified to build compliant mechanisms at insect scale. It demonstrates the straight line mechanism here by building the compliant micro-gripper.. This approach avoids the complexity of micro-fabricating flexures, by laser machining individual layers and then stacking individual layers to form a laminate. We demonstrate an end to end system complete with a solenoid actuator.The micro-gripper weighs 0.04 gms and the solenoid actuator weighs 0.2 grams.

5.1 Future Work

This work endeavored to build a tilable, sandwich flexures at microscopic scale as a basis to build steerable catheter tips and stents. It introduces compliance at the insect scale, opening up a host of possibilities to reduce part count and complicated sub-assemblies at insect scale.
Another avenue to explore would be the fabrication of curved flexures which would provide excellent directional stiffness and in-plane bendability for spherical application like a miniature HSA tube that can be built by tiling these flexures about an axis.

While this work focuses on using commercially available nitinol sheets to build flexures by laser cutting thin, long beams from aforementioned sheets. However, developing a machining system to machine nitinol tubes mimic the motion of steerable/flexible tip, would remove an additional layer of design complexity to building steerable catheter tips.

PUBLICATIONS

1. N. Elkunchwar, S. Chandrasekaran, V. Iyer and S. B. Fuller, "Toward battery-free flight: Duty cycled recharging of small drones," 2021 IEEE/RSJ International Conference on Intelligent Robots and Systems (IROS), 2021, pp. 5234-5241, doi: 10.1109/IROS51168.2021.9636087. [PDF]

2. Suvesha Chandrasekaran, Ian Good, Jeffrey I Lipton "Compliant Motor Driven Linear Bi-Layer Actuators" 2021 IEEE/RSJ International Conference on Soft Robotics (RoboSoft), 16:30-17:30, Paper Thu9Pos.17,[Link]

BIBLIOGRAPHY

[1] V. Iyer, M. Kim, S. Xue, A. Wang, and S. Gollakota, "Airdropping sensor networks from drones and insects," in *Proceedings of the 26th Annual International Conference on Mobile Computing and Networking*, ser. MobiCom '20. New York, NY, USA: Association for Computing Machinery, 2020. [Online]. Available: https://doi.org/10.1145/3372224.3419981

[2] M. Sitti, "Introduction, mobile microrobotics," *MIT Press, Cambridge, Massachusetts*, pp. 1–1, 2017.

[3] D. O. Popa and H. E. Stephanou, "Micro and mesoscale robotic assembly," *Journal of Manufacturing Processes*, vol. 6, no. 1, pp. 52–71, 2004, multiscale Fabrication/Integration. [Online]. Available: https://www.sciencedirect.com/science/article/pii/S1526612504700596

[4] N. El-Atab, R. B. Mishra, F. Al-Modaf, L. Joharji, A. A. Alsharif, H. Alamoudi, M. Diaz, N. Qaiser, and M. M. Hussain, "Soft actuators for soft robotic applications: A review," *Advanced Intelligent Systems*, vol. 2, no. 10, p. 2000128, 2020. [Online]. Available: https://onlinelibrary.wiley.com/doi/abs/10.1002/aisy.202000128

[5] H. E. Mulcahy and J. T. Cunningham, "A guidewire-assisted technique for removing retained biliary stents with rat-toothed forceps during endoscopic retrograde cholangiography," *Gastrointestinal Endoscopy*, vol. 53, no. 3, pp. 386–387, 2001. [Online]. Available: https://www.sciencedirect.com/science/article/pii/S0016510701704282

[6] Y. He, D. B. Wang, and Z. A. Ali, "A review of different designs and control models of remotely operated underwater vehicle," *Measurement and Control*, vol. 53, no. 9-10, pp. 1561–1570, 2020. [Online]. Available: https://doi.org/10.1177/0020294020952483

[7] C. P. Li Z, "Robotic endoscopy," *Visc. Med*, vol. 34, no. 1, pp. 45–51, 2018.

[8] J. I. Lipton, R. MacCurdy, Z. Manchester, L. Chin, D. Cellucci, and D. Rus, "Handedness in shearing auxetics creates rigid and compliant structures," *Science*, vol. 360, no. 6389, pp. 632–635, 2018.

[9] L. Chin, J. Lipton, R. MacCurdy, J. Romanishin, C. Sharma, and D. Rus, "Compliant electric actuators based on handed shearing auxetics," in *2018 IEEE International Conference on Soft Robotics (RoboSoft)*, 2018, pp. 100–107.

[10] L. L. Howell, *Handbook of Compliant Mechanisms*. John Wiley & Sons, Ltd, 2013.

[11] J. Pinskier and B. Shirinzadeh, "Topology optimization of leaf flexures to maximize in-plane to out-of-plane compliance ratio," *Precision Engineering*, vol. 55, pp. 397–407, 2019. [Online]. Available: https://www.sciencedirect.com/science/article/pii/S0141635918304641

[12] J. E. Correa, J. Toombs, N. Toombs, and P. M. Ferreira, "Laminated micro-machine: Design and fabrication of a flexure-based delta robot," *Journal of Manufacturing Processes*, vol. 24, pp. 370–375, 2016, sI: NAMRC. [Online]. Available: https://www.sciencedirect.com/science/article/pii/S1526612516300731

[13] J. P. Whitney, P. S. Sreetharan, K. Y. Ma, and R. J. Wood, "Pop-up book MEMS," *Journal of Micromechanics and Microengineering*, vol. 21, no. 11, p. 115021, oct 2011. [Online]. Available: https://doi.org/10.1088/0960-1317/21/11/115021

[14] K. Jayaram, J. Shum, S. Castellanos, E. F. Helbling, and R. J. Wood, "Scaling down an insect-size microrobot, hamr-vi into hamr-jr," 2020.

[15] T. YONEYAMA and C. KOBAYASHI, "12 - endodontic instruments for root canal treatment using ti–ni shape memory alloys," in *Shape Memory Alloys for Biomedical Applications*, ser. Woodhead Publishing Series in Biomaterials, T. Yoneyama and S. Miyazaki, Eds. Woodhead Publishing, 2009, pp. 297–305. [Online]. Available: https://www.sciencedirect.com/science/article/pii/B9781845693442500122

[16] C. Fu, Y. Guo, and M. Sealy, "A predictive model and validation of laser cutting of nitinol with a novel moving volumetric pulsed heat flux," *Journal of Materials Processing Technology*, vol. 214, no. 12, pp. 2926–2934, 2014. [Online]. Available: https://www.sciencedirect.com/science/article/pii/S0924013614002337

[17] V. Megaro, J. Zehnder, M. Bächer, S. Coros, M. Gross, and B. Thomaszewski, "A computational design tool for compliant mechanisms," *ACM Trans. Graph.*, vol. 36, no. 4, Jul. 2017. [Online]. Available: https://doi.org/10.1145/3072959.3073636

[18] P.York and R.Wood, "Nitinol living hinges for millimeter-sized robots and medical devices," *2019 International Conference on Robotics and Automation (ICRA)*, pp. 889–893, 2019.

[19] K. Jayaram and S. S. Joshi, "Development of a flexure-based, force-sensing microgripper for micro-object manipulation," *Journal of Micromechanics and Microengineering*, vol. 20, no. 1, p. 015001, nov 2009. [Online]. Available: https://doi.org/10.1088/0960-1317/20/1/015001

[20] S. Nah and Z. Zhong, "A microgripper using piezoelectric actuation for micro-object manipulation," *Sensors and Actuators A: Physical*, vol. 133, no. 1, pp. 218–224, 2007. [Online]. Available: https://www.sciencedirect.com/science/article/pii/S0924424706002305

[21] F. Székely and T. Szalay, *Design procedure of planar compliant microgrippers with flexural joints*, 12 2006.

[22] N. Doshi, B. Goldberg, R. Sahai, N. Jafferis, D. Aukes, R. J. Wood, and J. A. Paulson, "Model driven design for flexure-based microrobots," in *2015 IEEE/RSJ International Conference on Intelligent Robots and Systems (IROS)*, 2015, pp. 4119–4126.

[23] J. Herder, M. Horward, and W. Sjoerdsma, "A laparoscopic grasper with force perception," *Minimally Invasive Therapy & Allied Technologies*, vol. 6, pp. 279–286, 07 2009.

[24] C. Fu, M. Sealy, Y. Guo, and X. Wei, "Austenite–martensite phase transformation of biomedical nitinol by ball burnishing," *Journal of Materials Processing Technology*, vol. 214, no. 12, pp. 3122–3130, 2014. [Online]. Available: https://www.sciencedirect.com/science/article/pii/S0924013614002787

[25] X. Pei, J. Yu, G. Zong, and S. Bi, "Design of compliant straight-line mechanisms using flexural joints," *Chinese journal of mechanical engineering*, vol. 27, no. 1, pp. 146–153, 2014.